

RADIOCHEMISTRY AND RADIOPHARMACEUTICALS

N-13 L-Glutamate Uptake in Malignancy: Its Relationship to Blood Flow

Wolfram H. Knapp, Frantisek Helus, Hansjörg Sinn, Hermann Ostertag, Peter Georgi, Werner-E. Brandeis, and Arnim Braun

Institute for Nuclear Medicine, German Cancer Research Center, and University of Heidelberg, Heidelberg, West Germany

Studies on glutamate uptake, with special reference to perfusion, were carried out in 35 rats, each bearing one of five different tumor transplants; also in 15 rats after bone fracture, and in three rabbits. Single-pass extraction of N-13 glutamate was 85–93% in the VX2 tumor of the rabbit and in muscle. Bone fracture in rats caused a threefold increase of tracer uptake 2 days after the event. In tumor transplants, the tumor-to-muscle uptake ratio reached a maximum immediately following injection of the tracer. Comparing N-13 glutamate uptake with the retention of 1–121 microspheres, identical tumor-to-muscle ratios were found for three out of five tumor lines. Comparing the uptake with that of C-11 butanol (ten rats), a close correlation was observed throughout the range of tumor lines. The results suggested that glutamate uptake by malignant tumors is related to blood flow. In nine patients with malignant or benign lesions tumor-to-muscle uptake of N-13 glutamate and Tl-201 showed a linear correlation close to identity.

J Nucl Med 25: 989–997, 1984

The introduction of new therapeutic regimens has resulted in greatly increased quiescent intervals for a number of malignant tumors (1–3). These regimens utilizing adjuvant chemotherapy require documentation of tumor regression and progression. Hence there is growing interest in methods for in vivo assessment of metabolic activity in tumors. However, none of the radioagents commonly used for tumor imaging provides information on the viability of tumor cells and on their proliferative or invasive activity. Therefore, several investigators at medical cyclotron facilities have directed their attention to this need, using organic compounds labeled with C-11 or N-13 (4–11). Amino acids are predominantly used, since they are known to be involved in membrane and enzymatic alterations in malignancy (12). N-13 glutamic acid has received particular attention and has been evaluated in numerous patients in different clinical settings (7,9,11).

Use of N-13 L-glutamate has been encouraged because of its relatively simple synthesis (13). The first clinical observations were made in patients having bone tumors (4), in which high tracer uptake was found. Response to chemotherapy resulted in a parallel decrease of glutamate uptake (7).

It appears relevant to determine which physiological or metabolic factors cause an augmented N-13 glutamate uptake in malignant tumors. Thus it may be possible to understand better the value of N-13 glutamate scintigraphy for differential diagnosis in suspected malignant disease and for follow-up during therapy. In order to obtain this information, the activity uptake relative to perfusion, the kinetics of the N-13 activity in tumors, and the behavior of the tracer in nonmalignant lesions must all be considered.

MATERIAL AND METHODS

Tracer preparation. The N-13 activity was produced by the $^{16}\text{O}(\text{p},\alpha)^{13}\text{N}$ reaction according to the method described by Vaalburg and co-workers (14). For a 15-min irradiation with a beam current of 10 μA , typical

Received Nov. 25, 1983; revision accepted Apr. 9, 1984.

For reprints contact Prof. Dr. med. W. H. Knapp, Institut für Nuklearmedizin, Deutsches Krebsforschungszentrum, Im Neuenheimer Feld 280, D-6900 Heidelberg, West Germany.

yields were approximately 100 mCi $^{13}\text{NH}_3$, which corresponds to a production rate of 40 mCi/ $\mu\text{A}\cdot\text{hr}$.

In a buffered solution of $^{13}\text{NH}_3$ (pH 7.5–8.0), α -ketoglutarate was converted to L-glutamate by glutamic acid dehydrogenase (13). Following coagulation of the enzyme and elimination of unconverted $^{13}\text{NH}_4^+$ by cation-exchange chromatography, about 45 mCi N-13 L-glutamate were obtained in 3 ml solution with a specific activity of 590 mCi N-13/ μmole glutamate.

The radiopurity of N-13 L-glutamate was determined by thin-layer and high-pressure liquid chromatography. Samples of N-13 L-glutamate were routinely tested and found to be sterile. No adverse reactions have been observed to date in 115 patients examined with this tracer.

Labeled microspheres have been used for the invasive assessment of local blood flow. We chose I-121 as the radioactive label, since the physical properties of this positron emitter permit images to be produced that can be compared with those obtained with N-13. The most abundant gamma photons from I-121 decay are those of 212.5 keV (84.3%). Their energy is low enough so that the annihilation photons at 511 keV (abundance 14.5%) can be utilized.

Iodine-121 ($T_{1/2} = 2.12$ hr) was produced by the ^{122}Te (p, $2n$) ^{121}I reaction, using enriched Te-122 (15).

Microspheres were labeled by the following procedure:

Tin-tagged, 15–30- μm albumin microspheres were washed with citrate buffer (pH 4.5) to remove Sn^{2+} . The excess citrate was removed with distilled, pyrogen-free water. Labeling was then carried out in a double-chambered glass vial (oxidizing agent: NaIO_3 ; reaction time 15 min). The reaction medium was acidified with 0.5 M H_2SO_4 . After careful separation of unbound iodine, the labeling yield was about 70% (contamination with free iodine <0.1%).

In addition to the microsphere technique, the freely diffusible C-11 butanol (16) was used for blood-flow estimation. The synthesis has been described previously (17).

Animal experiments. Model for nonmalignant lesions. The left tibia was fractured in 15 male Sprague-Dawley rats, each weighing 225–250 g. One mCi N-13 L-glutamate was injected by tail vein in 0.5 ml saline solution 2–16 days after fracture. Following in vivo studies of activity distribution for 16 min, the animals were killed by air embolization. This was followed by in vitro measurements of radioactivity retained in the tibia, callus, and soft tissue. Five animals had regional blood-flow assessment. Forty minutes (= 4 half-lives) after the N-13 L-glutamate injection, these rats were given 1 mCi I-121-labeled microspheres, injected through a catheter into the aorta.

Tumor animals. Tumor transplants were derived from

spontaneous tumors arising in the BDX rat strain. The following lines have been investigated:

- BSp 25 (fibrosarcoma);
- BSp 41 (osteosarcoma);
- BSp 73 (adenocarcinoma of pancreas and ovary);
- BSp 130 (neurogenic sarcoma of uterus);
- BSp 141 (leiomyosarcoma of uterus).

Tumor-cell suspensions were injected i.m. into the hind legs of 35 BDX animals 2–3 wk before use. At this time, tumors measured 1–3.8 cm in diameter. Radionuclides were administered as in model for nonmalignant lesions.

Determination of single-pass extraction fraction. The fraction of labeled glutamate extracted by muscle and by the VX2 tumor of the rabbit during a single capillary transit was determined by a single-injection, external-registration technique first proposed by Sejrsen (18) and later developed and validated for the brain by Eichling et al. (19) and Raichle et al. (20). The extraction fraction (E) is measured by extrapolating the relatively slow clearance of the label from the tissue back to the maximum of the perfusion peak. With A = peak activity and B = extrapolated value at peak time, E equals B/A. Ten mCi of N-13 glutamate in 0.2 ml solution were rapidly injected into the A. femoralis of three rabbits bearing VX2 tumor transplants. The time-course of the activity in the hindquarters was recorded with a framing rate of 10 sec. Extrapolation of the tissue clearance was achieved by monoexponential least squares fitting of the slope between 5 and 15 sec after injection. Tc-99m-labeled serum albumin was used as an intravascular reference tracer.

Nuclide detection. The instrumentation required to take full advantage of the positron emission of N-13 is not yet in use in our laboratory. The animal studies are therefore based on single-photon detection with a commercial gamma camera equipped with a pinhole collimator. The field of view encompassed the trunk and the hind legs of the rat. The high-energy gamma rays were shielded with a lead plate 5 cm thick, positioned around the pinhole. Imaging of the rabbits was performed with a high-energy, parallel-hole collimator. A window setting of 20% was used to cover the 511-keV annihilation photons. Imaging of N-13 L-glutamate was begun immediately after injection. Images of I-121 microspheres were obtained 1–2 min after tracer application. Tissue preparations were measured with a well gamma spectrometer with Ge(Li) detector and automatic correction for decay. The probes were weighed with an accuracy in the range of 0.01 g.

Clinical studies. Forty patient investigations were included in the study, 31 on malignant disease, nine on benign lesions in the extremities. Each individual received 4–8 mCi N-13 L-glutamate by intravenous injection.

In 24 patients (27 investigations) quantitative positron

TABLE 1. UPTAKE RATIOS BETWEEN FRACTURED TIBIA AND CONTRALATERAL LEG (3-10 DAYS AFTER FRACTURE)

No	N-13 glu	I-121 μspheres
1	2.4	2.2
2	1.3	1.3
3	1.5	1.3
4	1.7	1.7
5	1.7	1.8
	Mean = 1.72	Mean = 1.66

imaging was performed with a nontomographic multi-crystal whole-body scanner (21) with a counting efficiency of 6,400 cps/μCi-cm². Total-body imaging required a scanning time of 8 min. Imaging was begun 3 min after the injection of the radiopharmaceutical, and the scans were repeated at 13 min. Scan data were collected on magnetic disk and were read by a computer connected to an interactive display system, corrected for sensitivity differences in the coincidence channels, for tissue absorption, and for the physical decay of the N-13 label during the scanning period. Absorption data were obtained from a transmission scan using a Ge-68/Ga-68 source.

Two-dimensional quantitation of regional activity was achieved by horizontal and vertical profiles (arms and thighs). Contralateral activity in regions having identical shape and size (joints) was also determined for comparison.

In 11 patients (13 investigations), the dynamic behavior of the N-13 label during the first 20 min after injection was studied using a commercial gamma camera equipped with a high-energy collimator. The framing

rate was 1 per 12 sec. In nine patients, N-13 glutamate imaging was preceded by Tl-201 dynamic scintigraphy (1-2 mCi) using the same framing rate as above. The initial activity distribution was assumed to represent regional distribution of flow (22).

RESULTS

Animal experiments. N-13 glutamate uptake by malignant tumors, normal tissue, and/or benign lesions has been studied in rats and rabbits. In three rabbits bearing hind-leg VX2 tumor transplants, the single-pass N-13 glutamate extraction fraction for both tumor and muscle ranged from 0.85 to 0.92.

Repair after fracture of the left tibia served as a model for nonmalignant activation of tissue proliferation. Following fracture of the rat tibia (N = 15), an augmented N-13 uptake was found for 18 days. The maximum relative uptake, compared against the contralateral side, was observed within the first 2 days. Uptake reached three times that of the control side.

In five rats with bone fracture, the N-13 glutamate investigation was followed by perfusion scintigraphy with I-121-labeled microspheres, injected into the aorta. After bone fracture in these rats, the mean local N-13 uptake was increased 1.7 times above the control region (Table 1). This was paralleled by an equal increase in microsphere fixation (mean = 1.65). The individual variation did not exceed 15%.

Homologous tumors implanted into a hind leg of 25 rats showed greatly different N-13 uptake. Tumor uptake ranged from 0.9 to 8.0 relative to the contralateral leg on an equal-volume basis. Each tumor type revealed a certain, sometimes characteristic, range of uptake values. The relative tumor activity remained constant from 2 to 15 min following injection, when average values for one tumor type are considered (Fig. 1). In 15

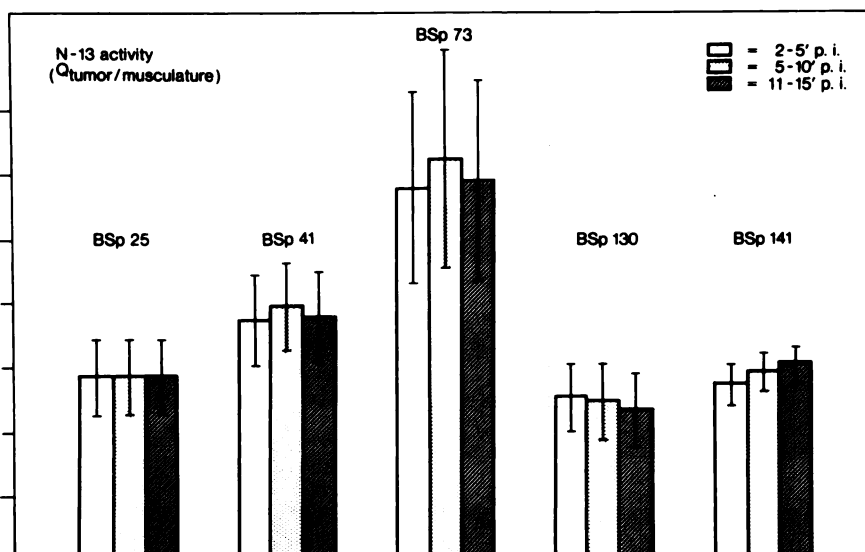


FIG. 1. N-13 L-glutamate uptake by tumors transplanted into hind leg of rat. Data were normalized to healthy opposite leg.

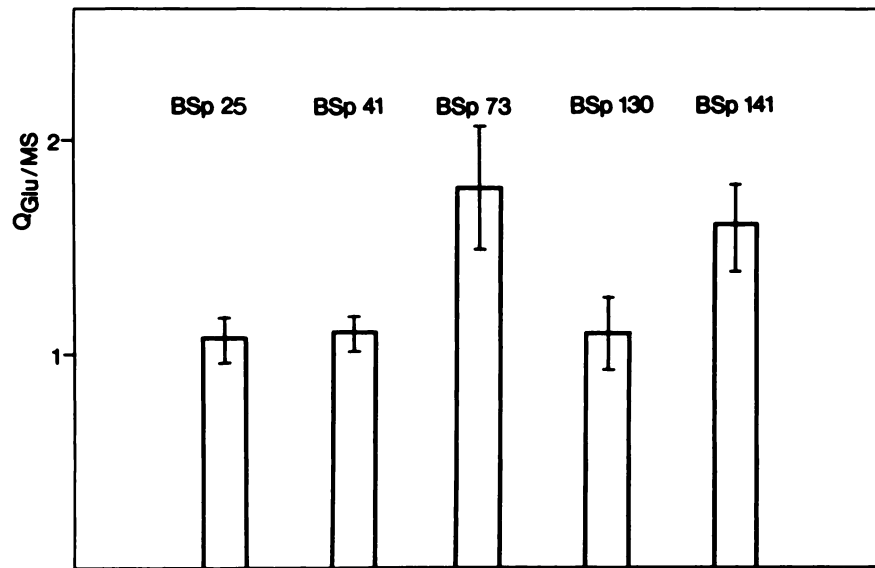


FIG. 2. Uptake ratios of N-13 glutamate and I-121 microspheres. Data are normalized to ratios obtained from control region.

tumor-bearing rats, the N-13 glutamate investigation was followed by the measurement of I-121 microsphere fixation. The average N-13 uptake value of these tumors was 2.1, while the I-121 activity averaged 1.7. The ratios between the uptake of N-13 glutamate and I-121 microspheres are shown for each tumor (Fig. 2). Considerable I-121 activity was noted in the lungs of some tumor-bearing rats, particularly in those with BSp 73 tumors. In order to evaluate the role of arteriovenous shunting, which may influence the fraction of microspheres retained in the BSp 73 tumor, the lung activity was measured in a well counter. Organs were excised 1 min after intraaortic injection of the microspheres in six tumor-bearing rats and five controls. The tumors (BSp 73) retained $(4.5 \pm 1.9)\%$ of the injected dose; $(13.5 \pm$

$5.9)\%$ was found in the lungs of tumor-bearing rats, and $(2.52 \pm 1.04)\%$ in the lungs of control animals ($t = 4.04$, $p < 0.005$). Because of this difference, an additional attempt to obtain blood-flow estimates was undertaken in 10 rats. Before the injection of I-121 microspheres, the initial uptake of C-11 butanol was assessed. There was good correlation between the tumor uptake of C-11

TABLE 2. UPTAKE RATIOS TUMOR-TO-CONTROL REGION FOLLOWING INJECTION OF N-13 GLUTAMATE AND TWO TRACERS FOR BLOOD-FLOW ESTIMATION

	N-13 glu	I-121 μ spheres	C-11 butanol
BSp 25	2.4	2.2	2.4
BSp 25	3.2	2.8	3.0
BSp 41	2.9	3.0	2.9
BSp 41	3.3	3.0	3.1
BSp 73	5.8	3.4	6.0
BSp 73	5.7	3.6	5.0
BSp 130	2.4	1.8	2.1
BSp 130	1.9	1.7	1.9
BSp 141	2.3	1.6	2.0
BSp 141	2.3	1.5	2.2
Means =	3.2	2.5	3.1
		$(r = 0.88)$	$(r = 0.98)$

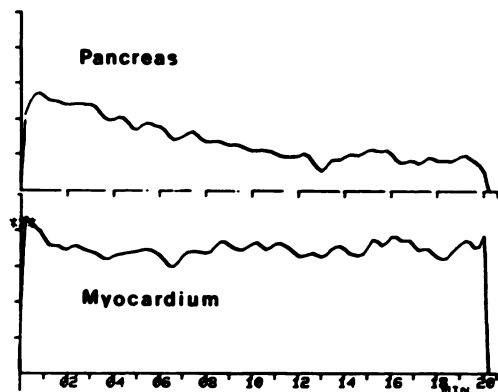
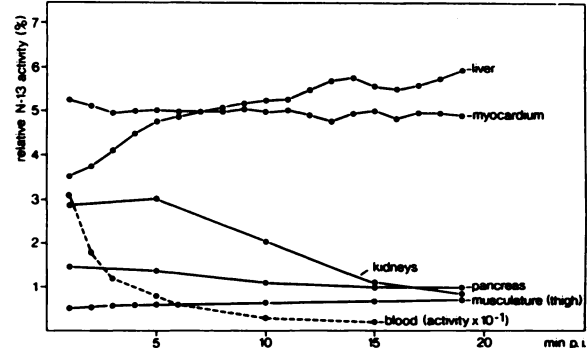


FIG. 3. Top: Time-activity curves, corrected for N-13 decay, from "regions of interest" over organs indicated. Bottom: Net time-activity curves for myocardium and pancreas. (Background was obtained from equal areas adjacent to organ.) Different handling of label is obvious.

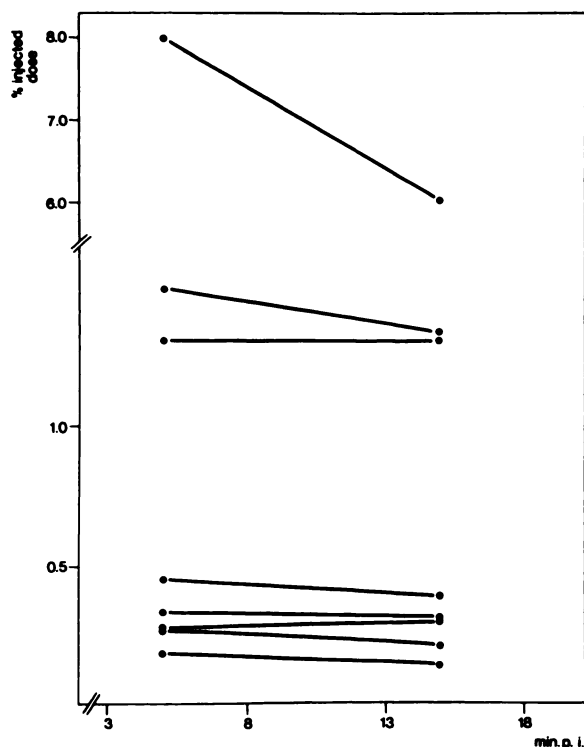


FIG. 4. Time course pattern of N-13 activity in human malignant tumors.

butanol and N-13 glutamate over the total range of tumor lines, including BSp 73 tumors (Table 2).

Patient studies. Kinetics of the label. Figure 3a shows a typical set of decay-corrected time-activity curves obtained from regions of interest, following injection of 5 mCi N-13 glutamate. Figure 3b shows replotted time courses of pancreatic and myocardial activity, after subtraction of background from an equal area adjacent to the respective organ. Three types of behavior were noted: A continuous rise in organ activity (liver), a steady state in the activity 3–20 min following injection (myocardium, muscles, and brain), and a rapid uptake followed by release of activity (pancreas and kidneys). The blood was cleared very rapidly (over 90% within 5 min). In most instances, human tumors showed constant levels of N-13 activity (Fig. 4) as determined with the positron scanner. Significant release of activity was observed in only two of eight human tumors (reticulosarcoma and metastasis of adenocarcinoma), both of which showed high initial uptake. The tumor-to-muscle ratio did not increase during the period of measurement in any of the 13 patient studies carried out with the gamma camera.

N-13 glutamate and Tl-201 uptake. In nine patients, local N-13 glutamate uptake was studied together with the initial Tl-201 uptake. The following lesions were investigated: osteosarcoma (five patients), soft-tissue sarcoma (one), metastasis from squamous cell carcinoma (one), osteofibroma (one), and Paget's disease (one). All of the lesions were located in the extremities. Their up-

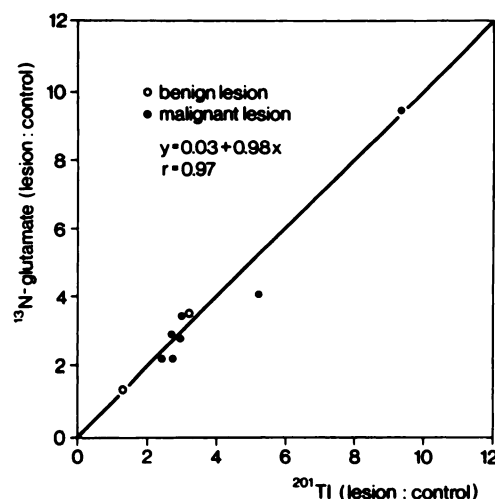


FIG. 5. Correlation between tumor-to-muscle uptake ratios for N-13 glutamate and Tl-201 in patients with malignant or benign lesions.

take was normalized to the uptake of a normal contralateral region containing muscle. The relative radionuclide uptake, thus derived, was plotted for Tl-201 and N-13 glutamate (Fig. 5). No different trends in the lesion-to-muscle uptake of the two tracers were found within a range of 1.3 and 9.5.

Clinical findings and N-13 glutamate uptake. A total of 40 N-13 glutamate uptake studies was made in patients suffering from various tumors or benign lesions located in the extremities.

All untreated malignant tumors showed an appreciably raised lesion-to-muscle uptake (2.8–12.0) and thus a 'positive' tumor image (Table 3). In patients with osteosarcoma, this tumor image often differed from the bone scan by the location and the size of the area involved. The reactive involvement of distal bone segments seen in the Tc-99m MDP scan was not paralleled by a similar N-13 activity uptake (Fig. 6). Moreover, there was no increased N-13 activity in physiologically acti-

TABLE 3. CLINICAL FINDINGS AND N-13 GLUTAMATE UPTAKE

Lesion	N	N-13 activity ratio tumor/control region
Malignant tumors, (untreated primary)	18	2.8–12.0
Malignant tumors treated (Grtr2 wk)	10	1.3–3.2
Metastases of carcinomas	3	2.0–8.0
Inflammatory diseases	4	1.0–2.8
Paget's disease	2	2.8, 3.5
Osteofibroma	2	1.0, 1.3
Bone cyst	1	1.0

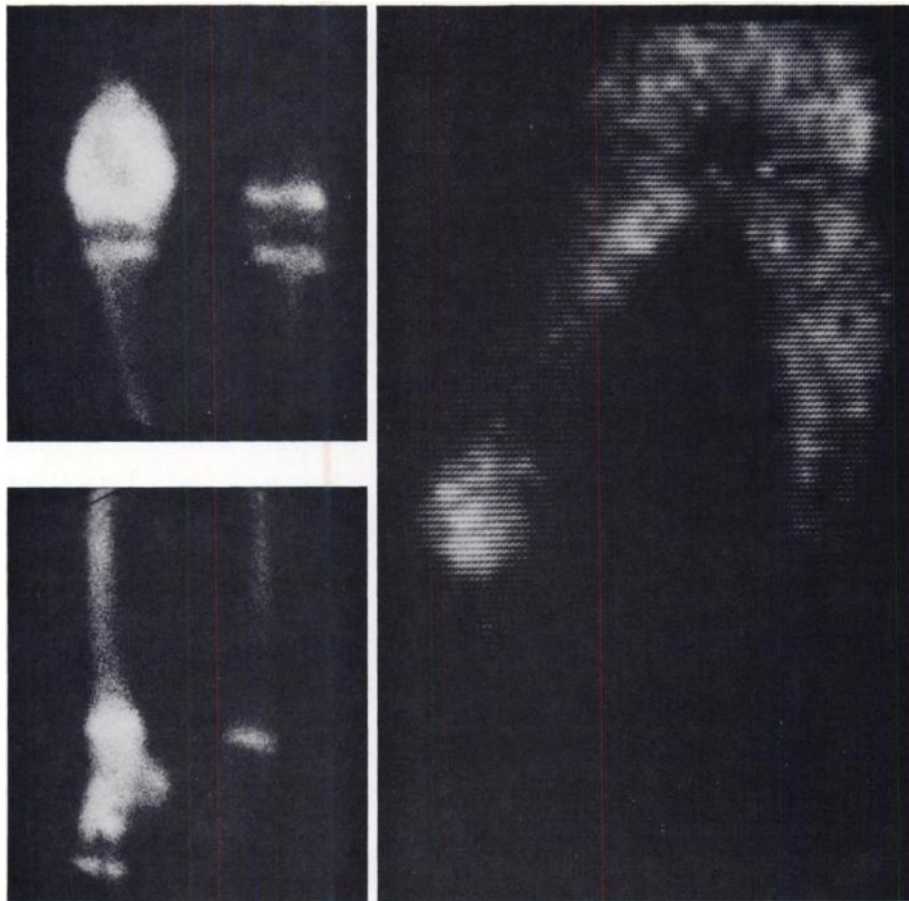


FIG. 6. Anterior scintigrams of osteosarcoma of right femur in 15-yr-old patient (anterior). Left: Tc-99m MDP shows relative uptake distal to tumor. Right: Intense N-13 glutamate uptake is confined to tumor; no visualization of epiphyses.

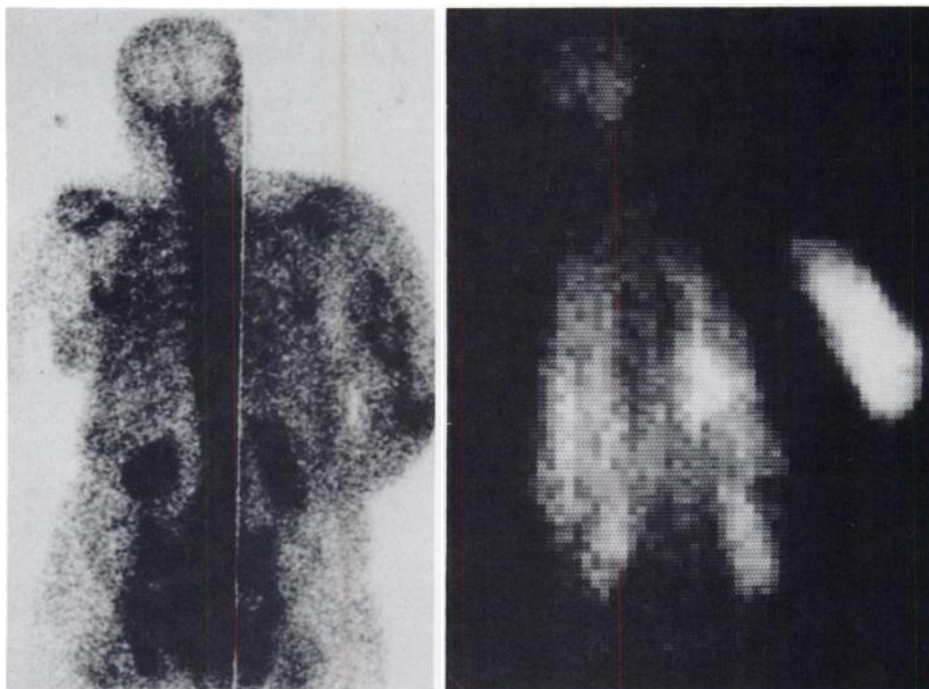


FIG. 7. Reticulosarcoma with destruction of left humerus. Left: Bone scintigram with Tc-99m MDP. Right: N-13 L-glutamate image.

vated bone metabolism (epiphyses in adolescence) (Fig. 6). In five out of nine tumors of nonosseous origin involving bone, N-13 uptake exceeded that of Tc-99m MDP (Fig. 7). Tumor-to-muscle uptake under treatment (>2 wk from the onset) ranged from 1.3 to 3.2.

Patients with benign bone lesions showed lesion-to-muscle uptake ratios from 1.0 to 3.5 (Table 3). Three out of eight patients failed to accumulate N-13 activity despite significant MDP accumulation.

DISCUSSION

Our clinical results confirm previously reported observations of increased uptake of intravenously injected N-13 glutamate in osteosarcoma and other malignant tumors (4,23-25). A connection has been shown between the decrease of N-13 uptake during therapy and the therapy response. This raises the questions: by which factors is the activity increase produced, and may it be observed in nonmalignant disease as well?

To evaluate the role of blood supply to the tumor in a model system, we sought to use a method for flow imaging that provides data comparable with those obtained in N-13 uptake measurements, i.e., counts per area and per unit of time, for the same tissue of interest relative to the same control region. We therefore made use of the fractional uptake of radioactive indicators for estimates of regional flow. According to this principle, Tc-99m-labeled microspheres have been used in various regional blood-flow studies (26-30). We substituted the positron emitter I-121 for the Tc-99m label in order to obtain the same counting efficiency and detection geometry as for N-13, using the pinhole collimator.

Regarding the microsphere measurements, it must be remembered that escape of particles occurs through physiologic or neoplastic arteriovenous shunts (31) and through widened tumor capillaries (32). While physiologic shunting of tracer amounts to only ~2-4% (31), the validity of the method for evaluation of nutritive perfusion has to be questioned in tumors.

Whereas increased N-13 uptake in fractured bone and some tumors was paralleled by a similar increase in perfusion as determined by MAA fixation, there was significant mismatch for the BSp 73 tumor. Arteriovenous shunting of the microspheres was suggested, since over 13% of the injected Tc-99m MAA was found in the lungs of BSp 73 tumor rats, on average, whereas control animals had only 2.5% of the activity in their lungs. Accordingly we used the freely diffusible tracer C-11 butanol (16), which resulted in different perfusion data in the BSp 73 tumor line. For butanol, an extraction ratio near 1.0 was assumed during the first arterial input, and the Sapirstein principle (33) was applied for flow estimation. With C-11 butanol, a close correlation between perfusion and N-13 glutamate uptake was noted for all tumor lines. These findings, and the high extraction

fraction found for N-13 glutamate, suggest that blood flow is the rate-limiting factor in N-13 glutamate uptake.

In order to extend the investigations on the relationship between perfusion and glutamate uptake to human tumors, it was essential to use a procedure that minimized discomfort to the patient. The use of Tl-201 avoided invasive tracer administration, and it allows the N-13 glutamate imaging to be performed rapidly subsequent to the study of the initial Tl-201 distribution. Again, the result of the correlation between the uptake of the two tracers suggests flow-limited uptake of N-13 glutamate in the lesions investigated.

The tissue level of the N-13 activity in tumors and normal tissue was relatively stable for the period of measurement, indicating a low rate of backdiffusion. Therefore, only a rapid turnover into the metabolic pool can account for the fact that uptake increases parallel with perfusion. From the data reported by Sauer et al. (34), it can be deduced that the glutamate fraction utilized does not exceed 25% of the total amount supplied to hepatomas and the Walker carcinoma. This appears in contrast to the statement that perfusion is the rate-limiting step in glutamate uptake. However, the different method of approach has to be considered. The cited report is based on steady-state arteriovenous concentration measurements. Consequently, substrate utilization is defined as net utilization, or substrate consumption minus production. Since our data were obtained after a single injection of the labeled substrate, they do not reflect the release of substrate synthesized *in vivo*.

Since our kinetic analysis of the N-13 label failed to show a protracted N-13 uptake phase, glutamate metabolism does not appear to have the potential to increase N-13 uptake in the tumors investigated. In transplanted rat tumors and in human tumors, we failed to find systematic differences in N-13 kinetics between tumor and musculature. In particular, tumor-to-muscle activity ratios showed a constant or decreasing, but never an increasing, tendency. This pattern contrasts with the N-13 kinetics in the liver, a major site of amino acid metabolism. Our findings are in agreement with studies on L [U-¹⁴C] glutamate in various tissues of rats bearing the Walker 256 carcinosarcoma (35).

Apart from perfusion and metabolism, the role of tissue transport must be considered. We know that the transport rate for amino acids may be increased in malignant cells (36,37). It appears unlikely, however, that differences in the transport mechanism would be able to elevate glutamate uptake. In order to show the relationship between uptake, transport rate, and flow, the following formula is used, by analogy with the concept of Renkin and Crone (38,39):

$$dA_i/dt = F/V \cdot C_p(t) [1 - \exp(-k_i V/F)],$$

where A_i = tissue activity concentration,
 F = flow, V = extracellular fluid space,

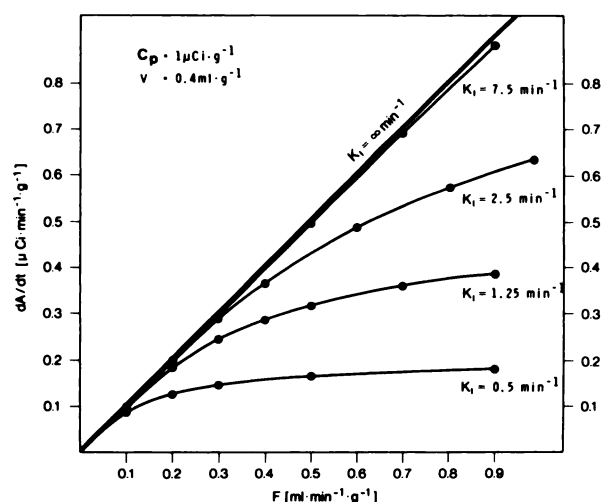


FIG. 8. Relationship between activity entering tissue per min and plasma flow, constant arterial plasma activity concentration, for different transport rate constants. Free diffusion between intravascular and interstitial fluid space is assumed. c_p = arterial plasma activity concentration, V = extracellular fluid space per gram tissue weight, A = activity per gram tissue weight, k_i = transport rate constant, F = plasma flow per gram tissue weight.

C_p = plasma activity concentration,
 k_i = transport rate coefficient for influx.

The third term on the right-hand side of the equation equals the extraction fraction (EF) of the tracer. Our EF measurements resulted in values from 0.85 to 0.92 for the normal musculature of the rabbit. Given typical values for muscle of 1/min (40) for flow per unit extracellular volume, and an EF of 0.90, the transport rate coefficient k_i becomes 2.3/min. As seen in Fig. 8, uptake—even at infinite k_i —would not differ essentially from uptake at $k_i = 2.5$ /min as long as flow remains below 0.6 ml/min-g. Only at very high flow rates may transport rate become a factor in determining uptake. The essence of the model is in agreement with our experimental results, which show that there are only minor differences between N-13 glutamate and that of the freely diffusible C-11 butanol.

The predominant contribution of local blood flow to N-13 glutamate uptake can explain the observations made under different clinical circumstances:

1. High N-13 activity in malignant bone tumors may be due to increased vascularization (41).
2. Activity decrease during tumor therapy may be paralleled by an obliteration of the vascular system (42,43).
3. N-13 accumulation was also found in some benign lesions like osteomyelitis and Paget's disease. Osteomyelitis may show vascular reactions to inflammatory mediators (44), and bones in Paget's disease are extremely vascular (45).

Our data, however, do not answer the question of whether N-13 glutamate uptake is also related to blood flow under antineoplastic therapy. According to the data

reported so far (7,24), the behavior of N-13 glutamate during therapy differs—as in untreated tumors—from that of Tc-99m pyrophosphate or MDP. Bone-seeking radiopharmaceuticals tend to show increased uptake in a number of bone tumors undergoing radiation plus chemotherapy (46), whereas response to therapy is usually accompanied by a decrease in N-13 glutamate uptake (23). Moreover, tumor recurrence in osteosarcoma is usually paralleled by an increase of N-13 glutamate, whereas bone-seeking radiopharmaceuticals show increased uptake in only a few of these instances, secondary to demineralization of bone (47).

Future investigations might be focused on determining whether vasoactive drugs or metabolic blocking by chemotherapeutic agents may influence the relationship between blood flow and glutamate uptake.

ACKNOWLEDGMENT

The authors are indebted to Mr. L. Gerlach for his technical assistance in the animal experiments, to Mrs. U. Mildner and Mrs. S. Dillenberger for their assistance in the investigation of patients, and to Mrs. E. Bender for her help in preparing the manuscript.

REFERENCES

1. JAFFE N, FREI E, TRAGGIS, et al: High-dose methotrexate with citrovorum factor in osteogenic sarcoma. *Progress Report II. Cancer Treat Rep* 61:675-679, 1977
2. ROSEN G, TAN C, SANMANEECHAI A, et al: The rationale for multiple drug chemotherapy in the treatment of osteogenic sarcoma. *Cancer* 35:936-945, 1975
3. ROSEN G, CAPARROS B, MOSENDE C, et al: Curability of Ewing's sarcoma and considerations for future therapeutic trials. *Cancer* 41:888-899, 1978
4. McDONALD JM, GELBARD AS, CLARK LP, et al: Imaging of tumors involving bone with ^{13}N -glutamic acid. *Radiology* 120:623-626, 1976
5. HÜBNER KF, ANDREWS GA, WASHBURN L, et al: Tumor location with 1-aminocyclopentane [^{11}C]carboxylic acid: Preliminary clinical trials with single-photon detection. *J Nucl Med* 18:1215-1221, 1977
6. WASHBURN LC, SUN TT, ANON JB, et al: Effect of structure on tumor specificity of alicyclic α -amino acids. *Cancer Res* 38:2271-2273, 1978
7. ROSEN G, GELBARD AS, BENUA RS, et al: N-13 glutamate scanning to detect the early response of primary bone tumors to chemotherapy. *Proc Am Assoc Cancer Res* 20:189, 1979
8. WASHBURN LC, SUN TT, BYRD BL, et al: 1-Aminocyclobutane [^{11}C]carboxylic acid, a potential tumor-seeking agent. *J Nucl Med* 20:1055-1061, 1979
9. GELBARD AS, BENUA RS, LAUGHLIN JS, et al: Quantitative scanning of osteogenic sarcoma with nitrogen-13-labeled L-glutamate. *J Nucl Med* 20:782-784, 1979
10. SOM P, ATKINS HL, BANDOYPADHYAY D, et al: A fluorinated glucose analog, 2-fluoro-2-deoxy-D-glucose (F-18): Nontoxic tracer for rapid tumor detection. *J Nucl Med* 21: 670-675, 1980
11. KNAPP WH, HELUS F, OBERDORFER F, et al: In-vivo assessment of amino acid transport in tumours by using ^{13}N - and ^{11}C -labelled compounds. In *Membranes in Tumour Growth*. Galeotti T, Neri G, Papa S, eds. Amsterdam-New York-Oxford, Elsevier Biomedical Press, 1982, pp 533-539

12. JOHNSTONE RM, SCHOLEFIELD PG: Amino acid transport in tumor cells. *Adv Cancer Res* 9:143-226, 1965
13. GELBARD AS, CLARKE LP, McDONALD JM, et al: Enzymatic synthesis and organ distribution studies with ^{13}N -labeled L-glutamine and L-glutamic acid. *Radiology* 116:127-132, 1975
14. VAALBURG W, KAMPHUIS JA, BEELING-VAN DER MOLEN HD, et al: An improved method for the cyclotron production of ^{13}N -labelled ammonia. *Int J Appl Radiat Isotop* 26:316-318, 1975
15. HELUS F, SILVESTER DJ, SAHM U, et al: Production of ^{121}I on the Heidelberg compact cyclotron and aspects of ^{121}I dosimetry. *Radiochem Radioanal Lett* 39:9-18, 1979
16. RAICHLE ME, EICHLING JO, STRAATMANN MG, et al: Blood-brain barrier permeability of ^{11}C -labeled alcohols and ^{15}O -labeled water. *Am J Physiol* 230:543-552, 1976
17. OBERDORFER F, HELUS F, MAIER-BORST W, et al: The synthesis of (1- ^{11}C)-butanol. *Radiochem Radioanal Lett* 53:237-252, 1982
18. SEJRSEN P: Single injection, external registration method for measurement of capillary extraction. In *Capillary Permeability*, Crone C, Lassen N, eds. New York, Academic Press, 1970, pp 256-260
19. EICHLING JO, RAICHLE ME, GRUBB RL, et al: Evidence of the limitations of water as a freely diffusible tracer in brain of the rhesus monkey. *Circulation Res* 35:358-364, 1974
20. RAICHLE ME, EICHLING JO, GRUBB RL, et al: Brain permeability of water. *Arch Neurol* 30:319-321, 1974
21. OSTERTAG H, KÜBLER W, KUBESCH R, et al: A multi-crystal positron scanner for quantitative studies with positron-emitting radionuclides. In *Medical Radionuclide Imaging 1980*, Vol 1, Vienna, IAEA, 1981, pp 29-39
22. BRADLEY-MOORE RP, LEBOWITZ E, GREENE MW, et al: Thallium-201 for medical use. II. Biologic behavior. *J Nucl Med* 16:156-160, 1975
23. GELBARD AS, CHRISTIE TR, CLARKE LP, et al: Imaging of spontaneous canine tumors with ammonia and L-glutamine labeled with N-13. *J Nucl Med* 18:718-723, 1977
24. REIMAN RE, HUVOS AG, BENUA RS, et al: Quotient imaging with N-13 L-glutamate in osteogenic sarcoma: Correlation with tumor viability. *Cancer* 48:1976-1981, 1981
25. HÜBNER KF, KING P, GIBBS WD, et al: Clinical investigations with ^{11}C -labeled amino acids using positron emission computerized tomography in patients with neoplastic diseases. In *Medical Radionuclide Imaging 1980*, Vienna IAEA-SM-247/90, 1981
26. KAPLAN WD, D'ORSI CJ, ENSMINGER WD, et al: Intra-arterial radionuclide infusion: A new technique to assess chemotherapy perfusion patterns. *Cancer Treat Rep* 62:699-703, 1978
27. BLEDDIN AG, KANTARJIAN HM, KIM EE, et al: $^{99\text{m}}\text{Tc}$ -labeled macroaggregated albumin in intrahepatic arterial chemotherapy. *Am J Roentgenol* 139:711-715, 1982
28. SIEGEL ME, WAGNER HN: Radioactive tracers in peripheral vascular disease. *Semin Nucl Med* 6:253-278, 1976
29. RODARI A, BONFANTI G, GARBAGNATI F, et al: Microsphere angiography in hepatic artery infusion for cancer. *Eur J Nucl Med* 6:473-476, 1981
30. KAPLAN WD, ENSMINGER WD, SMITH EH, et al: Intra-arterial hepatic infusion of Tc-99m-MAA: A predictive test of chemotherapeutic response of live tumors. *J Nucl Med* 20:675, 1979
31. RHODES BA, RUTHERFORD RB, LOPEZ-MAJANO V, et al: Arteriovenous shunt measurements in extremities. *J Nucl Med* 13:357-362, 1972
32. GULLINO PM: Extracellular compartments of solid tumors. In *Cancer*, Vol III, Becker FF, Ed. New York, Plenum, 1975, pp 327-354
33. SAPIRSTEIN LA: Regional blood flow by fractional distribution of indicators. *Am J Physiol* 193:161-168, 1958
34. SAUER LA, STAYMANN JW, DAUCHY RT: Amino acid, glucose, and lactic acid utilization in vivo by rat tumors. *Cancer Res* 42:4090-4097, 1982
35. NYHAN WL, BUSCH H: Metabolic patterns for L-glutamate- U^{14}C in tissues of tumor-bearing rats. *Cancer Res* 18:385-393, 1958
36. ISSELBACHER KJ: Increased uptake of amino acids and 2-deoxy-D-glucose by virus-transformed cells in culture. *Proc Natl Acad Sci US* 69:585-589, 1972
37. FOSTER DO, PARDEE AB: Transport of amino acids by confluent and nonconfluent 3T3 and polyoma virus-transformed 3T3 cells growing on glass cover slips. *J Biol Chem* 244:2675-2681, 1969
38. RENKIN EM: Transport of potassium-42 from blood to tissue in isolated mammalian skeletal muscles. *Am J Physiol* 197:1205-1210, 1959
39. CRONE C: The permeability of capillaries in various organs as determined by use of the indicator diffusion method. *Acta Physiol Scand* 58:292-305, 1963
40. BARCROFT H: Circulation in skeletal muscle. In *Circulation*, vol II (Handbook of Physiology), Hamilton WF, Dow PH, eds. Baltimore, Williams and Wilkins, 1974, pp 1353-1386
41. VOEGELI E, FUCHS WA: Arteriography in bone tumours. *Br J Radiol* 49:407-415, 1976
42. MÄNTYLÄ M, KUIKKA J, REKONEN A, et al: Regional blood flow in human tumours with special reference to the effect of radiotherapy. *Br J Radiol* 49:335-338, 1976
43. LINDBOM A, SODERBERG G, SPJPUT HJ: Osteosarcoma: a review of 96 cases. *Acta Radiol* 56:1-19, 1961
44. EDEIKEN J, HODES PJ: In *Roentgen Diagnosis of Diseases of Bone*, Vol 1, Baltimore, William and Wilkins, 1973, pp 578-661
45. BARRY HC: *Paget's Disease of Bone*, Edinburgh-London, Livingstone, 1969
46. FRANKEL RS, JONES AE, COHEN JA, et al: Clinical correlations of ^{67}Ga and skeletal whole-body radionuclide studies with radiography in Ewing's sarcoma. *Radiology* 110:597-603, 1974
47. MCKILLOP JH, ETCUBANAS E, GORIS ML: The indications for and limitations of bone scintigraphy in osteogenic sarcoma: a review of 55 patients. *Cancer* 48:1133-1138, 1981